A 16-Element Two-Dimensional Active Self-Steering Array Using Self-Oscillating Mixers

Grant S. Shiroma, *Student Member, IEEE*, Ryan Y. Miyamoto, *Member, IEEE*, and Wayne A. Shiroma, *Member, IEEE*

***Abstract*—A 16-element two-dimensional (2-D) retrodirective array using self-oscillating mixers (SOMs) is presented. SOMs allow for easier implementation of larger 2-D arrays by eliminating the complex local-oscillator (LO) feed structure. A 4 × 4 element retrodirective array using SOMs is demonstrated at an LO frequency of 7.68 GHz. Each element is phased locked at the LO frequency with an accompanying RF frequency isolation of 17.9 dB between adjacent horizontal elements and 22.2 dB between adjacent vertical elements. A −10-dBm external injection-locking signal is applied to reduce the phase noise of the 16-element array to −68.2 dBc/Hz at 10-kHz offset. Retrodirectivity is observed in the $\phi = 0°$, $\phi = -45°$, and $\phi = -90$ plane for scattering angles of $\theta = -15°$, $\theta = 0°$, and $\theta = +30°$.**

***Index Terms*—Antenna arrays, beam steering, microwave antenna arrays, phased arrays, retrodirective array, self-oscillating mixer (SOM).**

I. Introduction

RETRODIRECTIVE arrays have attracted a great deal of interest for their self-steering capability in wireless communications and solar power satellite systems (SPSs) [1]. These arrays have the unique property in that when the array is interrogated, the array automatically points its beam toward the interrogator. In contrast to conventional beam steering in a phased-array antenna, a retrodirective antenna is self-steering and does not require any phase shifters or digital signal processing. While a number of one-dimensional (1-D) retrodirective arrays have been recently demonstrated, very few two-dimensional (2-D) arrays have been published due to the added design complexity.

The Van Atta architecture [2] is the traditional method for realizing a retrodirective array, but 2-D retrodirectivity is difficult to achieve since elements from opposite sides of the array must be coupled through a complicated network of overlapping lines. 2-D retrodirectivity was demonstrated using four-wave mixing [3], but this architecture required four diode grids and two pumping sources.

The heterodyne technique [4] is another method for realizing retrodirective arrays. As shown in Fig. 1, this type of array employs mixers coupled to each antenna element. The mixers are designed so that an incoming RF signal of frequency f_{RF} mixes with a local oscillator (LO) at twice the RF frequency $2f_{\mathrm{RF}}$. The resulting IF signal is a phase-conjugated duplicate of the incoming RF source wave and reradiates in the direction of the source.

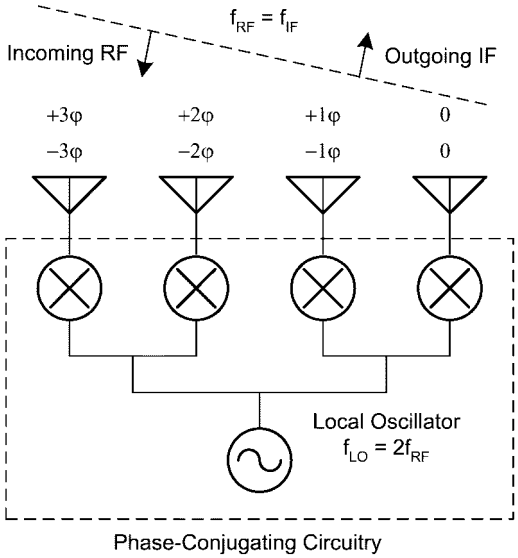

Fig. 1. Schematic of a phase-conjugation retrodirective array. The LO is provided from a corporate-fed transmission-line network.

For a phase-conjugating array to achieve retrodirectivity, the LO applied to each element must have the same phase. The conventional way of achieving this is to carefully design a corporate feed network so that the path lengths to each mixer are identical. However, feed networks become quite complicated for large 1-D linear arrays and severely limit the size of 2-D arrays; in fact, only one 2-D phase-conjugating array has appeared in the literature [5].

For efficient mixing, providing enough LO power to each element from a single source is challenging. Although a spatially fed LO [6] can eliminate the complex feed network, the amount of LO power delivered to the mixer is limited.

A solution to complex LO feed networks and LO power requirements is to eliminate the external LO source by basing the individual phase conjugating elements on self-oscillating mixers (SOMs). A retrodirective array can then by realized by phase locking the SOM elements at the LO frequency while isolating them at the RF frequency.

Although the idea of an SOM-based retrodirective array was proposed in [7], the first such array was demonstrated in [8], but this array radiated its LO in addition to the retrodirected IF signal and its usefulness was, therefore, limited. This paper presents the first 2-D SOM-based array that was specifically designed for retrodirective applications.

Manuscript received April 18, 2003. This work was supported in part by the National Science Foundation.

The authors are with the Department of Electrical Engineering, University of Hawaii at Manoa, Honolulu, HI 96822 USA.

Digital Object Identifier 10.1109/TMTT.2003.819779

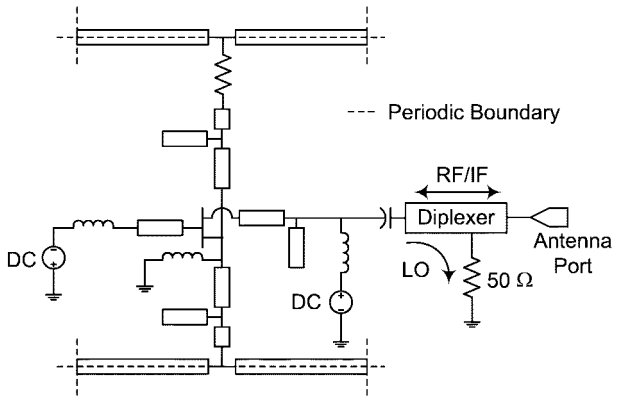

Fig. 2. Schematic of a phase-conjugating element using a SOM.

II. Phase-Conjugating Circuit Based on SOMs

The SOM and diplexer make up the unit cell shown schematically in Fig. 2. The circuitry is designed such that oscillation occurs at twice the RF frequency. This will allow the lower sideband of the second-order mixing product to be the phase conjugate of the RF signal. Since the size of the unit cell must be less than $\lambda_o/2$ at the RF frequency to avoid grating lobes, the antennas are mounted on a separate layer and connected to the phase-conjugating circuit through a via.

Phase locking of individual SOM elements is achieved by strongly coupling the source of each transistor through microstrip lines. For horizontal elements (i.e., elements parallel to the transistor's source leads), the length of the coupling line connecting each transistor's source lead is chosen to obtain a negative resistance at the desired oscillation frequency, while not exceeding the maximum unit-cell size. Vertical elements (i.e., elements parallel to the transistor's gate and drain leads) are coupled by a length of microstrip line that is a multiple of a wavelength at the LO frequency, while not exceeding the maximum unit-cell size. If the elements of the array are oscillating in phase, a virtual open is present at the periodic boundary. This allows the unit cell to be simulated by representing the microstrip lines that cross the periodic boundary as open-circuit stubs.

The unit-cell design approach is based on the assumption that all of the elements oscillate in phase [9]. However, in an array containing multiple elements, it is possible for other modes of oscillation to occur. A method of analyzing different oscillation modes of a 1-D array of strongly coupled oscillators is presented in [10]. Suppression of the unwanted modes is achieved by introducing a resistor at the midpoint of the lines coupling adjacent elements. A similar problem where adjacent horizontal elements would lock 180° out-of-phase was encountered during initial measurement of the prototype. By simulating a high-impedance voltage source at the LO frequency that is connected to the source of the transistor of each phase-conjugating element, we can obtain the voltage standing wave along different points of the coupling lines. If the sources are configured so that both the in-phase and 180° out-of-phase modes of oscillation are simulated, the results can be compared and a solution to attenuate the out-of-phase mode can be found. Introducing a resistor on the horizontal coupling line before the intersection of the vertical coupling line, as shown in Fig. 2, does little to affect to the in-phase mode since it is at the virtual open point. However, simulation shows that a resistor at this position attenuates the 180° out-of-phase mode.

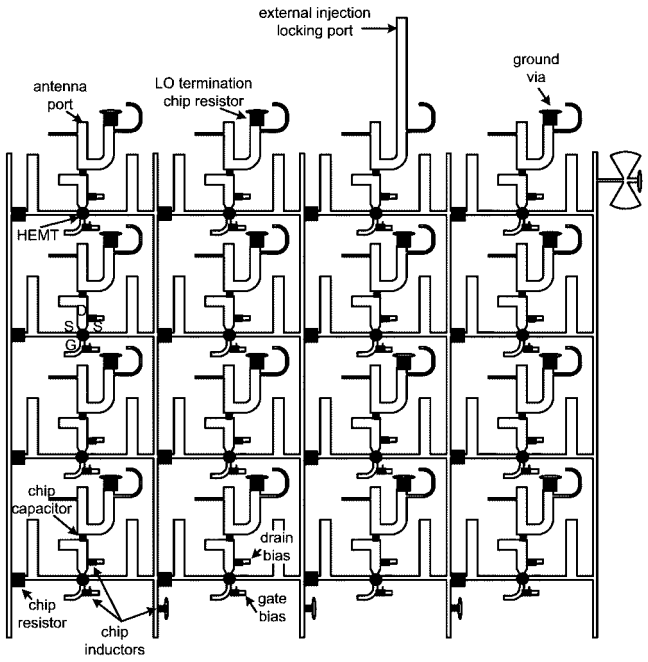

Fig. 3. 4×4 element phase-conjugating circuit using SOMs.

While the elements of the array are strongly coupled at the LO frequency, a retrodirective array requires that each element be isolated at the RF/IF frequency. Single-stub RF bandstop filters are employed on each side of the transistor on the horizontal coupling lines to provide isolation between adjacent elements at the RF/IF frequency.

The oscillation frequency of the SOM is determined by optimizing the length of the open-circuit stub attached to the transistor's gate in conjunction with the matching network at the drain to achieve a negative resistance of $-150\ \Omega$ in accordance to the one-third rule [11].

For the mixing operation, the RF and IF is applied and extracted from the drain of the transistor. A diplexer comprised of single-stub bandstop filters is inserted to reduce unwanted LO radiation by isolating the antenna port from the LO termination. At the LO frequency, the output port of the SOM only sees the 50-Ω load, while only the antenna is visible at the RF/IF frequency.

The prototype 16-element phase-conjugating SOM array is shown in Fig. 3. The circuit is fabricated on an RT duroid 5880 substrate (thickness 0.7874 mm, $\varepsilon_r = 2.2$). The active devices are Agilent ATF-36077 ultra-low-noise pseudomorphic high electron-mobility transistors (pHEMTs). Gate and drain biasing is applied through chip inductors, while chip capacitors provide dc blocking. Subminiature A (SMA) connectors are mounted on the ground plane side of the substrate through drilled holes to allow a connection to the RF/IF port of the diplexer. This configuration simplifies testing of individual phase-conjugating elements. An SMA connector is also

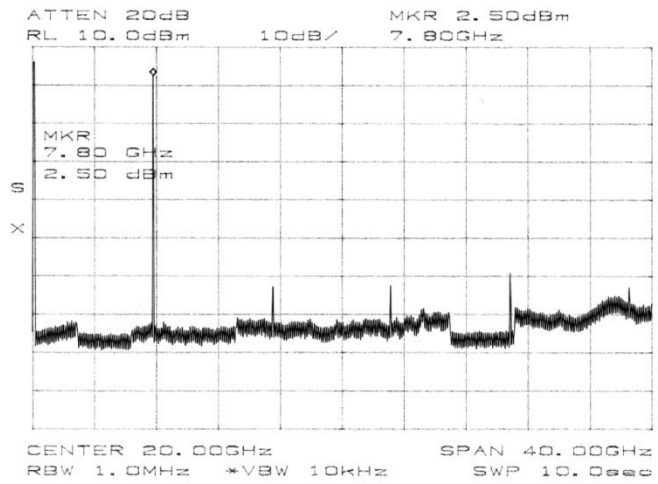

Fig. 4. LO spectrum generated by the SOM circuit.

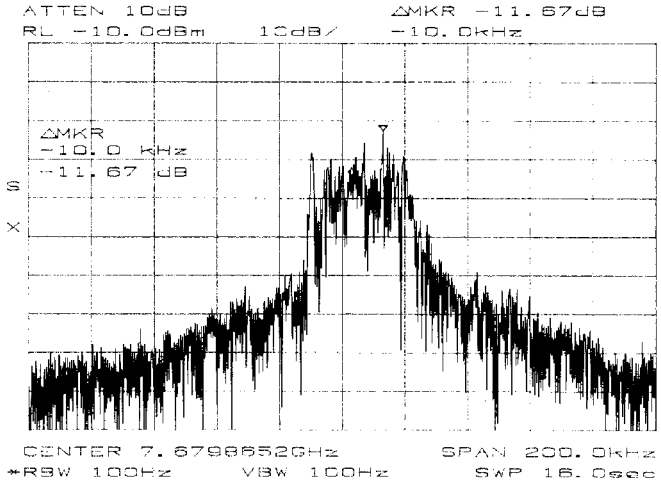

Fig. 5. Spectrum of LO without external injection locking.

mounted to one element at the edge of the array in place of the LO termination to serve as an external injection locking port. Unwanted modes of oscillation are suppressed by inserting a 50-Ω resistor on the horizontal coupling line, as depicted in Fig. 2. This resistor value was chosen based on availability, but any reasonable value should be appropriate since the in-phase mode is unaffected by this resistor. All vertical coupling lines were dc grounded to negate the effect of the mode-stabilizing resistance on the transistor biasing.

For proper operation of the SOM array, the SOMs have to be turned on at the same time. This is achieved by using a common dc supply for all the SOMs. The transistors are biased at class A. The circuit is optimized so that it oscillates at 8.0 GHz. Fig. 4 shows the measured spectrum of the oscillation signal taken at the external injection-locking port. The measurement shows that the SOM elements are phased locked with a fundamental oscillation frequency of 7.80 GHz. Discrepancies between the simulated and measured oscillation frequency is due to the insertion of the chip resistor used for mode stabilization. While an ideal resistor of zero length would not affect the in-phase mode, the resistor used has a finite length that was not compensated for in this prototype. At the fundamental frequency, an oscillation power of 3.8 dBm is measured for a single SOM element.

To evaluate the effects of external injection locking, the phase noise of the oscillation signal is measured. The injection-locking signal is applied at the edge of the array through the external injection-locking port, while the LO leakage signal is monitored through the RF/IF port at the opposite side of the 16-element array. An HP 83650L signal generator is used as the injection locking source since it is capable of providing a low phase-noise signal of -80 dBc/Hz at 10-kHz offset. Fig. 5 shows the phase noise of the oscillation signal without external injection locking to be -11.7 dBc/Hz at 10-kHz offset. When a -10-dBm external injection locking signal at 7.680 GHz is applied, the phase noise reduces to -68.2 dBc/Hz at 10-kHz offset, as shown in Fig. 6. Besides reducing the LO phase noise, the injection-locking signal could also be used as a source for frequency or phase-modulation schemes.

Next, mixing performance is evaluated by applying an external RF signal to the SOM circuit through a directional coupler

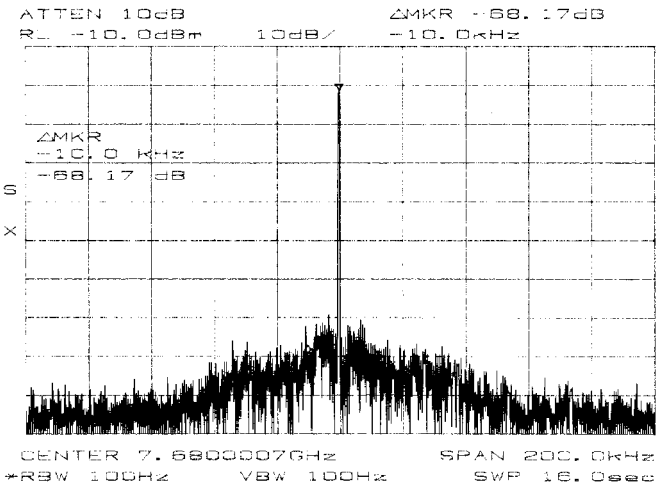

Fig. 6. Spectrum of LO with external injection locking.

[12]. The phase-conjugated IF signal is measured using a spectrum analyzer from the coupled port of the directional coupler. At an RF frequency of $f_{\rm LO}/2$, the measured conversion gain is -20.6 dB. Low conversion gain is expected since the SOM was only optimized for oscillation according to the one-third rule without taking the mixing performance into account.

For an array of phase-conjugating elements to properly function as a retrodirective array, each element must be isolated from one another. The RF isolation between elements is measured by injecting an RF signal into an element and measuring the coupled signal at an adjacent element. At an RF frequency of 3.84 GHz, the RF isolation between adjacent horizontal elements is 17.9 and 22.2 dB between adjacent vertical elements.

III. 2-D Retrodirective Array

A 4 $\times$ 4 array of radiating-edge fed patch antennas, shown in Fig. 7, is fabricated such that the element spacing is equal to the phase-conjugating array unit cell. At an RF frequency of 3.840 GHz, the element spacing in the H-plane is 3.48 cm (0.464 λ_o) and 2.90 cm (0.386 λ_o) in the E-plane. RT duroid 5880 (thickness 0.7874 mm, $\varepsilon_r = 2.2$) is the substrate used

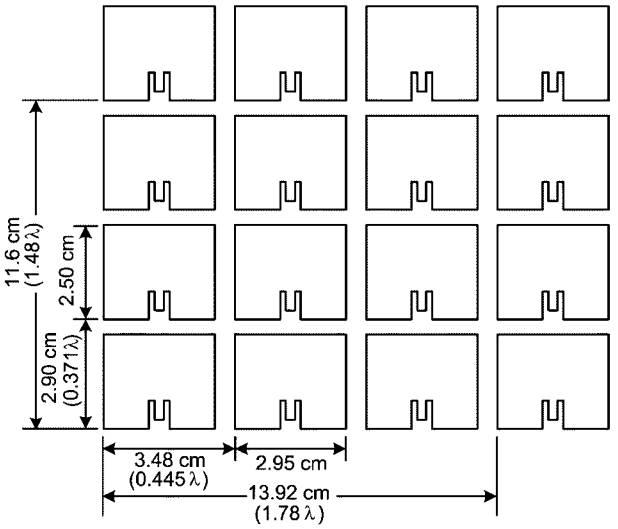

Fig. 7. 4×4 element patch antenna array.

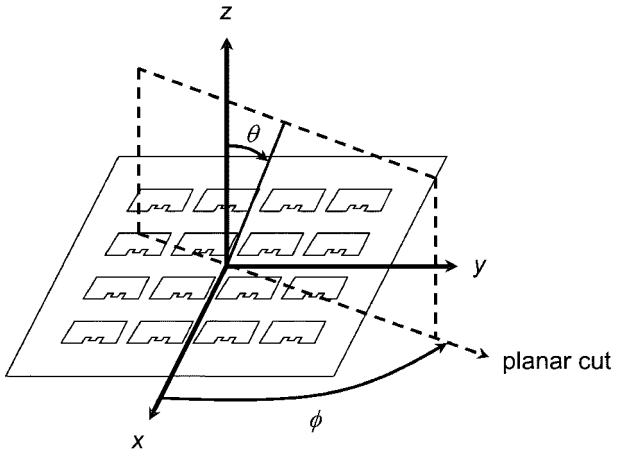

Fig. 8. Coordinate system used for radiation pattern measurements.

for the patch-antenna array. SMA connectors are mounted on the ground-plane side of the substrate through drilled holes to allow a connection to be made to individual patch antennas. This configuration allows testing and tuning of individual antenna elements and facilitates easy interfacing with the phase-conjugating circuit.

Retrodirectivity is verified through bistatic and monostatic radiation patterns. A -10-dBm external injection locking signal at 7.680 GHz is applied to reduce the LO phase noise. Applying a RF signal at 3.839 GHz results in an IF signal of 3.841 GHz, thereby allowing both signals to be monitored on the spectrum analyzer. Fig. 8 shows the coordinate system used in the radiation pattern measurements. The array is placed in the x–y-plane so that the E-plane is in the x–z-plane, while the H-plane lies in the y–z-plane. In the bistatic measurement setup shown in Fig. 9, the position of the RF transmitting horn is fixed while the IF receiving horn is mounted on a computer-controlled rotational arm that scans from $\theta = -60°$

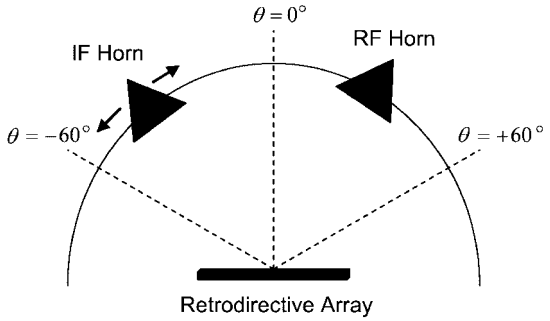

Fig. 9. Setup for measuring the bistatic radiation pattern.

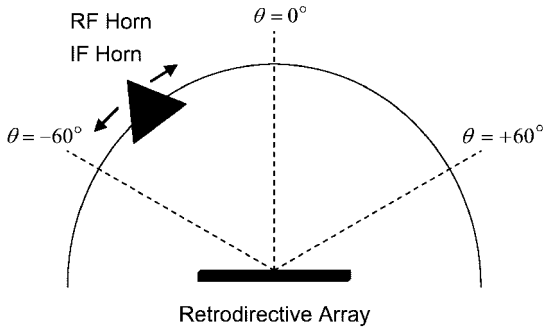

Fig. 10. Setup for measuring the monostatic radiation pattern.

to 60°. The bistatic radar cross section (RCS) is given by the following:

$$\sigma_{\text{bistatic}}(\theta,\theta_0,\phi,\phi_0) = \frac{\lambda_0^2}{4\pi} G_c D_{\text{patch}}(\theta_0,\phi_0) \times D_{\text{patch}}(\theta,\phi) D_{\text{array}}(\theta,\theta_0,\phi,\phi_0) \quad (1)$$

where θ_0 and ϕ_0 are the RF source angles, G_c is the circuit gain, D_{patch} is the element directivity, and D_{array} is the directivity of the array given by the following:

$$\begin{aligned} D_{\text{array}}(\theta,\theta_0,\phi,\phi_0) &= \frac{|AF(\theta,\theta_0,\phi,\phi_0)|^2}{U_0(\theta_0,\phi_0)} \\ &= \frac{4\pi\,|AF(\theta,\theta_0,\phi,\phi_0)|^2}{\int_0^{2\pi}\int_0^{\pi} |AF(\theta',\theta_0,\phi',\phi_0)|^2 \sin\theta' d\theta' d\phi'}. \end{aligned} \quad (2)$$

In the bistatic measurement, the radiation pattern of the array is fixed as the position of the RF source (i.e., θ_0, ϕ_0) is fixed. This means that the integration of the array factor U_0 is constant. Therefore, the directivity of the array simply depends on the angle θ where the IF receiving horn is located. The normalized bistatic pattern is given by the following:

$$\sigma'_{\text{bistatic}}(\theta,\phi)|_{\theta_0,\phi_0} = \frac{\left|\text{AF}(\theta,\phi)|_{\theta_0,\phi_0}\right|^2 D_{\text{patch}}(\theta,\phi)}{\max\left(\left|\text{AF}(\theta,\phi)|_{\theta_0,\phi_0}\right|^2 D_{\text{patch}}(\theta,\phi)\right)} \quad (3)$$

where AF is the array factor. As the array factor has the maximum value at the incoming angle of the RF signal, the main

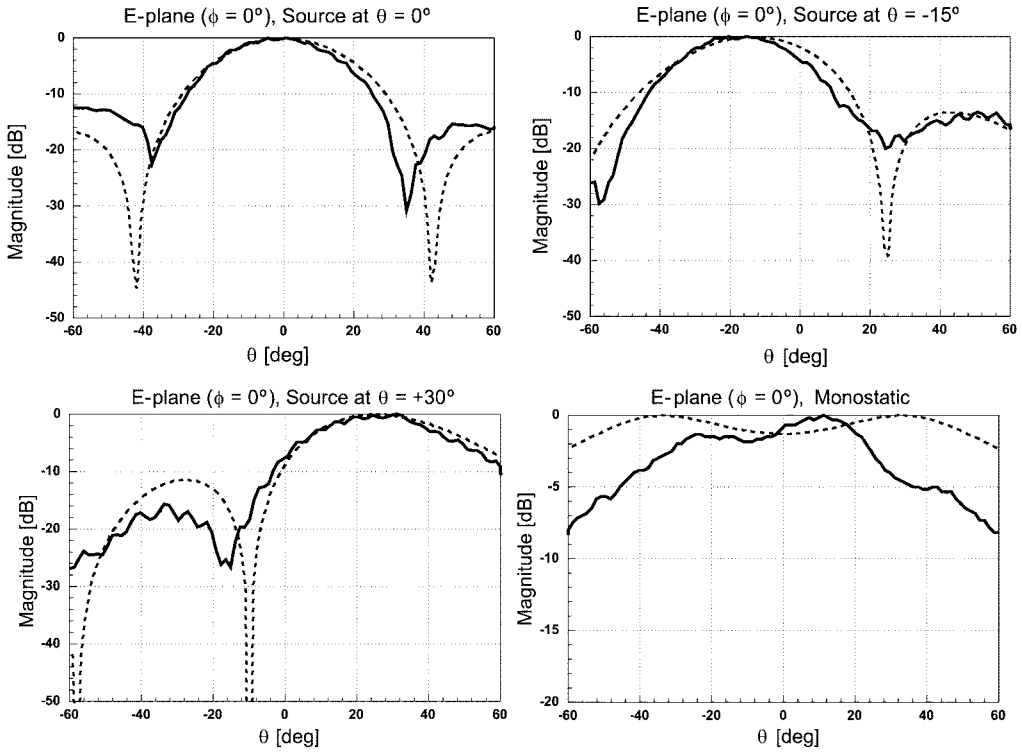

Fig. 11. E-plane ($\phi = 0°$) bistatic radiation patterns for scattering angles of $\theta = 0°$, $\theta = -15°$, and $\theta = +30°$ and monostatic radiation pattern.

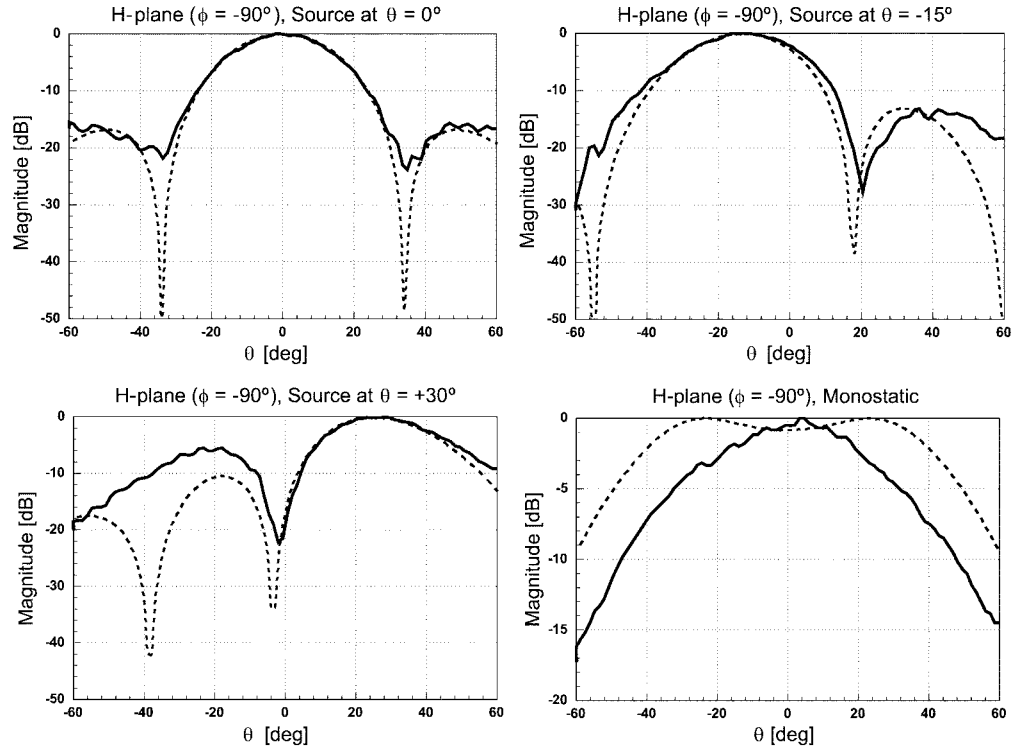

Fig. 12. H-plane ($\phi = -90°$) bistatic radiation patterns for scattering angles of $\theta = 0°$, $\theta = -15°$, and $\theta = +30°$ and monostatic radiation pattern.

lobe of the bistatic radiation pattern should point in the direction of the source. Another common measurement is the monostatic measurement, as shown in Fig. 10. In this measurement, the RF and IF antennas are collocated and moved together ($\theta = \theta_0$, $\phi = \phi_0$) to measure the radiation from the array, thus the IF receiving antenna is always in the direction of the main lobe. Both the RF and IF horns are mounted on a computer-controlled rotational arm and scans together $\theta = \pm 60°$. The monostatic RCS pattern is given by the following:

$$\sigma_{\text{monostatic}}(\theta, \phi) = \frac{\lambda_0}{4\pi} G_c D^2_{\text{patch}}(\theta, \phi) D_{\text{array}}(\theta, \phi). \quad (4)$$

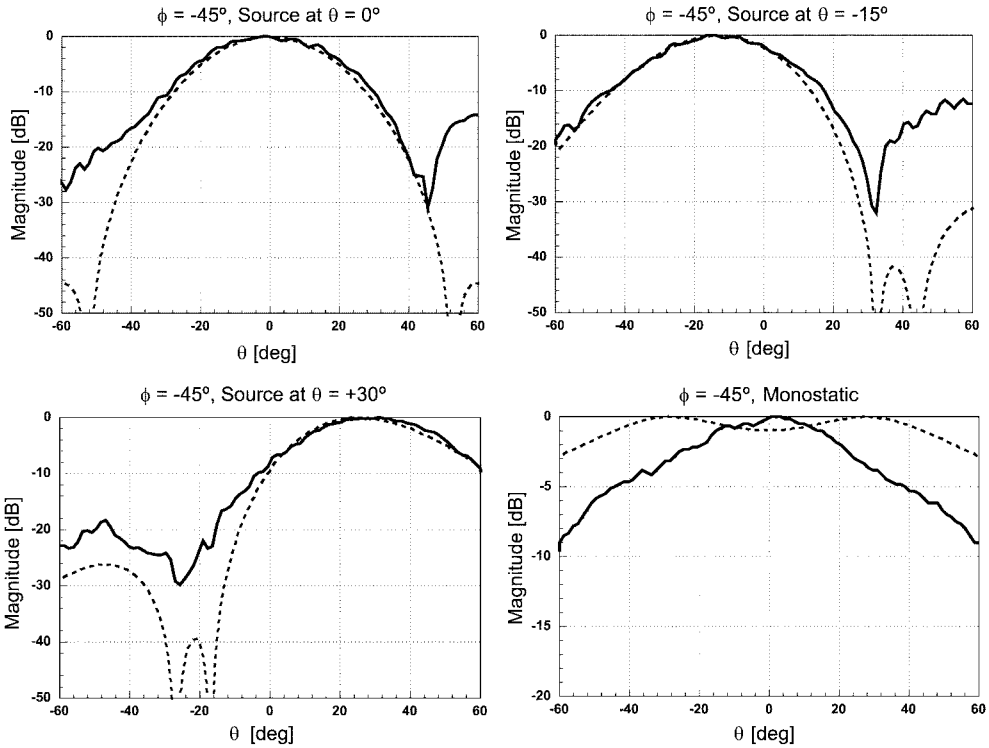

Fig. 13. $\phi = -45^\circ$ bistatic radiation patterns for scattering angles of $\theta = 0^\circ$, $\theta = -15^\circ$, and $\theta = +30^\circ$, and monostatic radiation pattern.

In the monostatic measurement, the radiation pattern varies as θ, ϕ changes. This implies that the array directivity at the peak is not constant, and it depends on the scanning angle, i.e., the position of the RF and IF horns, θ, and ϕ [13], [14]. The normalized monostatic pattern is given by the following:

$$\sigma'_{\text{monostatic}}(\theta,\phi) = \frac{\dfrac{D^2_{\text{patch}}(\theta,\phi)}{U_0(\theta,\phi)}}{\max\left(\dfrac{D^2_{\text{patch}}(\theta,\phi)}{U_0(\theta,\phi)}\right)}. \tag{5}$$

Figs. 11 and 12 show the measured and theoretical bistatic radiation patterns and the monostatic radiation pattern in the $E(\phi = 0^\circ)$ and $H(\phi = -90^\circ)$ planes. The bistatic radiation patterns are measured with RF sources at $\theta = 0^\circ$, $\theta = -15^\circ$, and $\theta = +30^\circ$. The theoretical patterns are obtained based on (3) and (5). The measured bistatic and monostatic radiation patterns confirm retrodirectivity in both of the principle planes. By combining both E- and H-plane bistatic measurements, we can confirm 2-D retrodirectivity.

The measured and theoretical bistatic radiation patterns and monostatic radiation pattern in the $\phi = -45^\circ$ plane, as shown in Fig. 13, are unique only to a 2-D retrodirective array. The measured bistatic radiation patterns with RF sources at $\theta = 0^\circ$, $\theta = -15^\circ$, and $\theta = +30^\circ$, and the monostatic radiation pattern, confirm 2-D retrodirectivity.

IV. Conclusion

A 16-element 2-D retrodirective array using SOMs has been presented. A 4 × 4 retrodirective array using SOMs is demonstrated at an LO frequency of 7.68 GHz. Each element is successfully phased locked at the LO frequency while 17.9 dB of isolation between adjacent horizontal elements and 22.2 dB of isolation between adjacent vertical elements is measured at the RF frequency. A −10-dBm external injection locking signal is applied to reduce the phase noise of the 16-element array to −68.2 dBc/Hz at 10 kHz. Retrodirectivity is successfully observed in the $\phi = 0^\circ$, $\phi = -45^\circ$, and $\phi = -90$ planes for scattering angles of $\theta = -15^\circ$, $\theta = 0^\circ$, and $\theta = +30^\circ$. Retrodirective arrays using SOMs do not require complex LO feed networks, thereby allowing the realization of larger 2-D arrays.

References

[1] R. Y. Miyamoto and T. Itoh, "Retrodirective arrays for wireless communications," *IEEE Microwave Mag.*, pp. 71–79, Mar. 2002.

[2] L. C. Van Atta, "Electromagnetic reflector," U.S. Patent 2 908 002, Oct. 6, 1959.

[3] W. Ding, S.-T. C. Lei, and M. P. DeLisio, "A retrodirective diode grid array using four-wave mixing," in *IEEE MTT-S Int. Microwave Symp. Dig.*, Phoenix, AZ, May 2001, pp. 1851–1854.

[4] C. Y. Pon, "Retrodirective array using the heterodyne technique," *IEEE Trans. Antennas Propagat.*, vol. AP-12, pp. 176–180, Dec. 1964.

[5] C. W. Pobanz, "Time-varying active antennas: Circuits and applications," Ph.D. dissertation, Dept. Elect. Eng., Univ. California at Los Angeles, Los Angeles, CA, 1997.

[6] W. E. Forsyth and W. A. Shiroma, "A retrodirective antenna array using a spatially fed local oscillator," *IEEE Trans. Antennas Propagat.*, vol. 50, pp. 638–640, May 2002.

[7] S. C. Yen and T. H. Chu, "Phase conjugation array using subharmonically injection locked self-oscillating mixers," in *IEEE AP-S Int. Symp Dig.*, July 2001, pp. 692–695.

[8] D. M. K. Ah Yo, W. E. Forsyth, and W. A. Shiroma, "A 360° retrodirective self-oscillating mixer array," in *IEEE MTT-S Int. Microwave Symp. Dig.*, Boston, MA, June 2001, pp. 813–816.

[9] S. Kawasaki and T. Itoh, "Quasi-optical planar arrays with FET's and slots," *IEEE Trans. Microwave Theory Tech.*, vol. 41, pp. 1838–1844, Oct. 1993.
[10] S. Nogi, J. Lin, and T. Itoh, "Mode analysis and stabilization of a spatial power combining array with strongly coupled oscillators," *IEEE Trans. Microwave Theory Tech.*, vol. 41, pp. 1827–1837, Oct. 1993.
[11] G. Gonzalez, *Microwave Transistor Amplifiers Analysis and Design*. Englewood Cliffs, NJ: Prentice-Hall, 1997.
[12] R. Y. Miyamoto, Y. Qian, and T. Itoh, "An active retrodirective transponder for remote information retrieval-on-demand," *IEEE Trans. Microwave Theory Tech.*, vol. 49, pp. 1658–1662, Sept. 2001.
[13] R. C. Hansen, *Phased Array Antennas*. New York: Wiley, 1997.
[14] W. L. Stutzman and G. A. Thiele, *Antenna Theory and Design* New York, 1998.

Grant S. Shiroma (S'00) received the B.S. degree from the University of Hawaii at Manoa, in 2002, and is currently working toward the M.S. degree in electrical engineering at the University of Hawaii at Manoa.

His research interests include microwave circuits and phased arrays.

Ryan Y. Miyamoto (S'97–M'03) received the B.S. degree in physical electronics from the Tokyo Institute of Technology, Tokyo, Japan, in 1997, and the M.S. and Ph.D. degrees in electrical engineering from the University of California at Los Angeles, in 1999 and 2002 respectively.

Since 2002, he has been with the University of Hawaii at Manoa. His research interests include phased arrays, microwave receivers, and mobile communication systems.

Dr. Miyamoto was the recipient of the Second Place Prize in the Student Paper Contest of the 2001 IEEE Microwave Theory and Techniques Society (IEEE MTT-S) International Microwave Symposium (IMS), and the International Symposium on Antennas and Propagation (ISAP) Paper Award presented at the 2000 International Symposium on Antennas and Propagation.

Wayne A. Shiroma (S'85–M'87) received the B.S. degree from the University of Hawaii at Manoa, in 1986, the M.Eng. degree from Cornell University, Ithaca, NY, in 1987, and the Ph.D. degree from the University of Colorado at Boulder, in 1996, all in electrical engineering.

In 1996, he joined the University of Hawaii at Manoa, where he is currently an Associate Professor of electrical engineering. He was also a Member of the Technical Staff at Hughes Space and Communications, El Segundo, CA. His research interests include microwave and millimeter-wave integrated circuits and antennas.

Dr. Shiroma is a member of the IEEE Microwave Theory and Techniques Society (IEEE MTT-S) Administrative Committee (AdCom).